Scintillation Detector Calibration and Optimization for Neutral Atom Trap for Beta Decay

Fall 2022 CO-OP Work Term Report

Melisa Ozen

University of Ottawa

Abstract

At TRIUMF's Neutral Atom Trap for Beta Decay, we investigate the time-reversal symmetry in beta decays of trapped atoms. For a four-momentum final state, such as during radiative beta decay, the correlation of the three momenta from beta-neutrino-gamma coincidences could indicate a violation of the time-reversal symmetry. Such a study requires high-precision measurements. Here, we report the calibration and optimization studies for scintillation detectors with Silicon Photomultiplier (SiPM) readout for the detection of decay products of radioactive trapped atoms. The effect of a light guide attached to a plastic scintillator on the energy resolution of the scintillation detector was investigated. We also designed a housing for the same detector for installation around our atom trap and reported the changes in the energy resolution with the assembly of the new design and compared two different types of SiPMs. Energy resolution as good as 9.3% around 1 MeV was achieved with the housing design and a certain type of SiPM for the plastic detector. Furthermore, we used a neutron source, AmBe to calibrate our plastic detector at a relatively higher energy. The plastic detector was coupled with two GAGG (Gadolinium Aluminium Gallium Garnet) gamma-ray detectors. Through triple gamma-ray coincidences between the three detectors, the double escape peak at 3.42 MeV was isolated. Finally, the apparatus symmetry was tested on recoil ion coincidences with gamma-ray decays during two radioactive test runs with trapped 45K atoms. The improvements in the signal-to-noise ratio for the coincident particle pair spectrum between the two runs were discussed for future time-reversal violation studies.

Keywords: radiation detection, scintillation detectors, gamma rays, time-reversal symmetry

Table of Contents

1 Introduction

Time-reversal symmetry breaking in weak interactions could indicate physics beyond the Standard Model. We require high-precision methods to observe the correlation of three momenta that could suggest a symmetry violation, such as the beta-neutrino-gamma coincidences during a radiative beta decay [1]. In this report, we present our calibration and optimization studies for scintillation detectors to achieve high-precision measurements of the decay products to investigate time reversal violation (TRV) in radiative beta decay.

The first part of this report serves as a reminder of the background theory of the TRV which is the main motivation for this research. In the second part, we report the improvements on our plastic scintillation detectors such as a light guide attachment, a new readout board and a housing design and we discuss their effect on the energy resolution at around 1 MeV.

In the third part, we introduce a method for higher energy calibrations for plastic scintillation detectors using a neutron source, AmBe, that emits gamma rays at 4.44 MeV. We explore a new calibration method by coupling a plastic detector with two inorganic Gadolinium Aluminium Gallium Garnet (GAGG) detectors to isolate the double escape peak at 3.42 MeV through energy cuts around the annihilation radiation from the GAGG detectors and a triple gamma-ray timing cut between the detectors. We discuss the nature of the tail on the left-hand side of the double escape peak with a GEANT4 simulation and determine the energy resolution of the plastic to be 11.5 ± 0.8% at 3.42 MeV.

Finally, we present our coincident pair spectrum for the recoil ion coincidences with gamma rays for a trapped radioactive potassium isotope, 45K which is important to test the apparatus symmetry. We report a better signal-to-noise ratio in our spectrum after improvements in our atom trap.

2 Background Theory

The violation of time-reversal symmetry could indicate physics beyond the electroweak interaction predictions of the Standard Model. We investigate the interactions between the decay products in a radiative beta decay by observing their momenta [1]. A scalar triple product of momenta $p_1 \cdot p_2 \times p_3$ flips sign with the sign of time [2]. A non-zero value of the scalar triple product would indicate a violation of the time-reversal symmetry; however, it is prevented by momentum conservation for normal beta decay:

$$^{37}\mathrm{K} \rightarrow {}^{37}\mathrm{Ar} + \beta^{+} + \nu$$

$$p_\nu = -p_\beta - p_{recoil} \Rightarrow p_{recoil} \cdot p_\beta \times p_\nu = 0$$

The construction of a three-momenta state from a four-momentum final state could resolve this problem. Therefore, we look for a three-momenta state from a four-momentum final state in radiative beta decay to investigate the time-reversal symmetry breaking [2]:

$$^{37}\mathrm{K} \rightarrow {}^{37}\mathrm{Ar} + \beta^{+} + \nu + \gamma$$

$$p_\beta \cdot p_\nu \times p_\gamma$$

3 Organic Scintillation Detector Improvements

3.1 Experimental Setup

The goal of our detector improvement studies was to design and optimize two organic scintillation detectors to be installed on the top and at the bottom of our atom trap, inside a mounting flange with a Si detector placed at the bottom of the flange. We conducted test experiments with a 30-mm-thick BC408 plastic scintillator with 88 mm diameter attached to a 40-mm-thick light guide with 88 mm diameter (Fig. 1a). The bottom of the scintillator is narrower with 10 mm in height and 58 mm in diameter to accommodate the geometry of the flange. The sides of the light guide were wrapped with around 3-4 layers of PTFE (a.k.a Teflon), whereas the scintillator part was wrapped in about 10 layers of PTFE (0.075 mm thickness per layer). Nitrocellulose was reported to have a higher reflection coefficient as compared to 4 layers of ACE Teflon tape by Janecek [3]. We covered the bottom of the scintillator with only one layer of nitrocellulose with 0.12 mm thickness to minimize the energy loss of the incident beta particles. We attached two layers of thick Teflon sheet (0.75 mm thickness per layer) on top of the scintillator (the readout side) and placed a thin layer of gel between the readout and the scintillator (or the light guide) surface to minimize the light loss between the scintillator and the readout mediums due to the difference in refractive indexes compared to air.

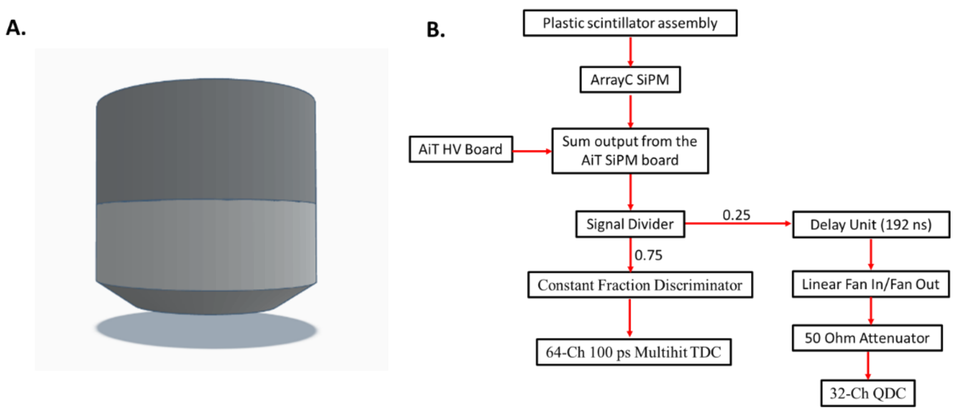

Fig. 1. Plastic scintillation detector setup. **A.** 3D model of the plastic scintillator attached to the light guide. **B.** Schematic diagram of the data acquisition system for the detector.

The data acquisition system for the plastic detector is described in Fig. 1b. Our readout was SensL ARRAYC-60035-64P-PCB 57x57mm Silicon Photomultiplier (SiPM) and that was coupled with a readout board by AiT Instruments, ABL-ARRAY64PH to sum and amplify the signals from the SiPM array. Our SiPM array was biased with a high voltage evaluation board by AiT Instruments, model HV80EVB, at 29-30 V. The gain of the sum signal could be adjusted with a knob on the SiPM readout board, from 0 up to 2, as well as the coupling type (AC or DC) and the sign of the signal. For all our experiments, we used DC coupling and a negative sum signal since the input signal needs to have a negative sign for the QDC.

For our initial experiments with the scintillator attached to the light guide, we used a 50Ω splitter to split the sum signal from the SiPM readout board into two in order to access both the energy and the timing information. For the rest of our test experiments, we replaced the 50Ω splitter with a ¼ - ¾ signal divider and added a CAEN Fan In/Fan Out for the ¼ of the signal to adjust the DC offset after delaying it by 192 ns. The signal was later attenuated with a 50Ω attenuator before the QDC. The ¾ of the signal was adjusted with a RoentDek Constant Fraction Discriminator (CFD) which is typically used to improve the time response of electronic signals from secondary emission devices [4]. Optimized pulses were then read by our TDC.

For our test experiments, we investigated the effect of the presence of the light guide, gain from the readout board, and the signal attenuation on the energy resolution of our scintillation detector.

3.2 Light Guide and Gain Adjustments

The energy resolution of our plastic scintillation detector was determined through one of our radioactive sources, 207Bi. Plastic scintillators are low-Z materials, therefore, they have very low photopeak detection efficiency which makes them ineffective for gamma-ray detection. 207Bi is a gamma-ray source that also emits internal conversion (IC) electrons. During internal conversion for high-Z isotopes like 207Bi, the high energy radiation from the decaying isotope interacts with an electron from the outer shells instead of radiating a gamma ray, causing the electron to be ejected from the atom [5]. These electrons can be detected by the organic scintillation detectors as energetic peaks. We used the IC electron peak from the K, L and M shells of 207Bi combined at around 1 MeV. A Gaussian model was fitted to the experimental data to determine the energy resolution for our test experiments.

The light guide was designed to increase the number of photons detected and the correct geometry for the light guide was determined through GEANT4 simulations. We investigated the energy resolution of our plastic scintillator attached to the 40-mm-thick light guide. The sum signal from the SiPM readout board was split in half and attenuated up to 0.1 of the signal to prevent saturation in our QDC. We determined the energy resolution to be 21.0 ± 0.7% for the IC electrons of 207Bi at 1 MeV. This was a significantly worse result as compared to the energy resolution determined for our initial tests with a similar plastic scintillator (not attached to a light guide) with 35 mm thickness, 90 mm diameter and the same SiPM array. 11.8 ± 0.5% of energy resolution was determined for that detector. After these results, we detached our plastic scintillator from the light guide and repeated our measurements with the same experimental setup. We measured an energy resolution of 11.2 ± 0.3%, similar to what we had found for our initial tests with the 35-mm-thick scintillator. We suspect light loss from the sides of the light guide that resulted in fewer photon counts and poorer energy resolution. This might have been caused by thinner PTFE wrapping around the light guide as compared to the scintillator side. We decided to keep our scintillator detached from the light guide.

Our QDC registers the energy of the photons emitted through our scintillator as a limited number of channels in our data acquisition system, with a certain offset and gain. After the detachment of the light guide, we were no longer in our desired energy range of 0.5 – 5 MeV, possibly due to higher gain caused by more light collection. To calibrate the gain of our detector, we started using ¼ of the sum signal instead of ½ for the QDC and decreased the gain on the SiPM readout board from 1 to 0.25. After these adjustments, the energy resolution at 1 MeV was determined as 14.6 ± 0.4%.

We were also worried that higher energy photons like cosmic background pulses higher than 5 MeV were getting saturated by our SiPM readout board. We replaced the board with a new AiT board, AB1TR-G100-ARRAYJ64P, which was essentially the same except with reduced transimpedance by a factor of 5. This provided us with 5 times less gain as compared to the first SiPM readout board we had used. However, this resulted in even worse energy resolution for our plastic scintillator: 19.1 ± 0.5%. We also noticed that we were able to detect the cosmic background with the first SiPM readout board as well and that the board was not saturating at higher photon energies. Therefore, we decided to switch back to the first readout board.

3.3 Scintillator Housing Design

We needed a new design for our scintillation detectors to be able to insert all the parts inside a mounting flange without hurting the delicate Si strip detector at the bottom of the flange. We also needed to keep all the detector parts together, especially against gravity for the installation at the bottom of the atom trap. Hence, we designed a scintillator housing using a 3D modeling tool called COMSOL. Figure 2 shows the 3D scintillator housing design from the side. Some pieces were purchased such as the Ø3" Thorlabs lens tube, ensuring a light seal around the SiPM array. Some other pieces were ordered and machined like the Teflon piece between the scintillator and the strip detector, the Teflon washer between the top of the scintillator and the SiPM array, a steel and another titanium pieces on top of the housing to lock every piece together and gently push the SiPM array towards the surface of the scintillator through the lens tube.

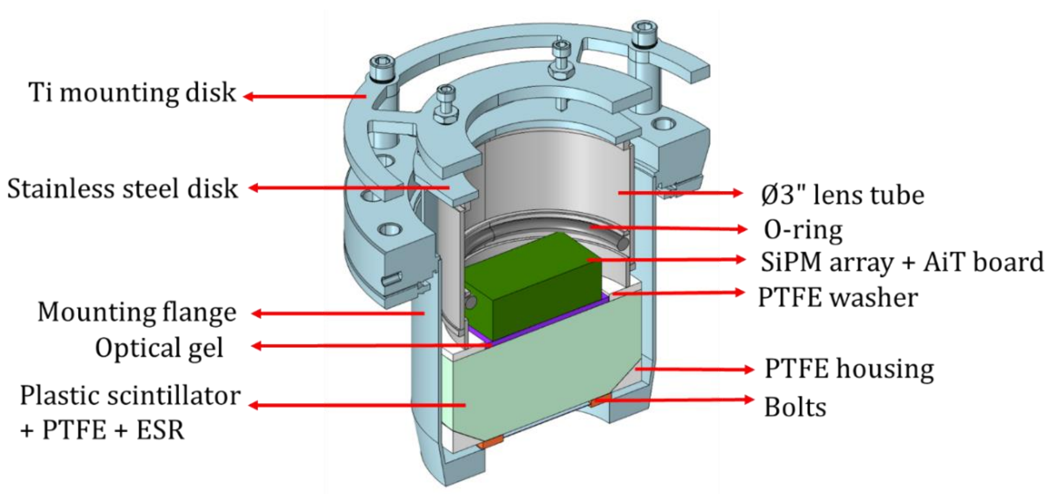

Fig. 2. The new plastic scintillator detector assembly with the housing design inside the mounting flange. The plastic scintillator is wrapped with ~10 layers of PTFE and one layer of ESR. This figure lacks another layer of Teflon sheet and ESR on top of the PTFE washer.

The main differences between this design and the detector assembly we used for the previous tests are an additional layer of ESR (enhanced specular reflector) on top of the PTFE wrappings around the scintillator, a Teflon washer instead of 2 layers of Teflon sheet on top of the scintillator (the readout side), another layer of Teflon sheet and ESR layer on top of the Teflon washer for additional reflection around the SiPM array. We also designed the housing in a way to push the SiPM array gently through the lens tube against the gel on the scintillator. This might have prevented the presence of air between the gel and the scintillator which could minimize the light loss in the air due to differences in refractive indexes, resulting in more light collection by the SiPM array.

We assembled two scintillation detectors in the same way. Their only difference was the SiPM arrays used. The detector that was installed on top of the atom trap had SensL ARRAYJ-60035-64P-PCB (or J-type) 50x50mm SiPM, whereas the bottom one had SensL ARRAYC-60035-64P-PCB (or C-type) 57x57mm SiPM. These SiPMs are both 8x8 arrays manufactured by the same company with similar sizes. However, the individual arrays on the C-type SiPM are more dispersed as compared to the J-type. The C-type is also composed of less numbers of microcells. These factors might cause small differences in performance, resulting in fewer photon collection by the C-type. However, we could not find any performance comparisons published by the manufacturing company, therefore, we only report our test results for our scintillation detector assemblies.

We determined that the detector with the J-type SiPM and 0.5 gain on the SiPM readout board had 9.3 ± 0.3% energy resolution at 1 MeV. At the same energy, the detector with the C-type SiPM and the same gain on the SiPM readout board had 10.2 ± 0.4% energy resolution. However, we had to further calibrate the detector with the J-type SiPM for our desired energy range of 0.5 – 5 MeV and decreased the gain on the SiPM readout to 0.375, which resulted in 10.1 ± 0.3% resolution. In the end, both of our detectors had similar energy resolutions at similar energy ranges. From our experiments, we deduced that decreasing the gain on the summing board significantly impacts the energy resolution of the scintillation detectors and should be calibrated carefully according to the desired energy range in the DAQ.

We note that biasing the SiPMs at 29V instead of 30V is also a useful way to calibrate the energy range on the DAQ since the energy resolution does not change between 29V and 30V bias voltages (but it might at lower voltages due to decreased photon detection efficiency).

4 High-Energy Calibrations for the Organic Detector

4.1 AmBe Experiments

We used a neutron source, AmBe, to calibrate our plastic scintillation detector at a relatively high energy of 3.42 MeV. The experimental setup for the calibrations is described in Fig. 3. We coupled the plastic scintillation detector with two inorganic Gadolinium Aluminium Gallium Garnet (GAGG) scintillation detectors.

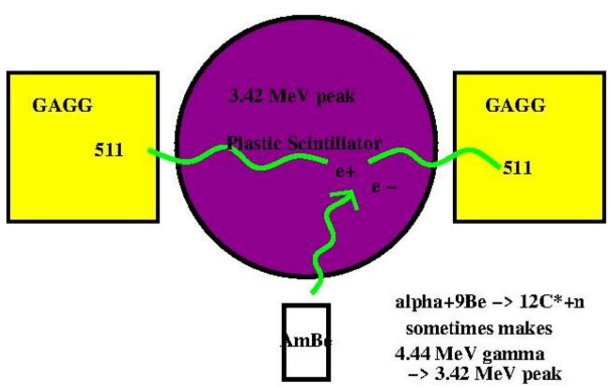

Fig. 3. Schematic for the AmBe experiment showing the decay process and the GAGG detectors placed at the sides of the plastic detector. This figure lacks the polyethylene block between the plastic scintillator and the AmBe source.

Our calibration source decays into gamma rays at 4.44 MeV. Implementing triple gamma-ray timing coincidences between the three detectors significantly helped us get rid of the neutrons that were dominating the energy spectrum of the plastic detector and isolate the gamma rays instead. Then, by isolating the 511 keV annihilation radiation peaks in the GAGG detectors, we were able to observe the double-escape peak at 3.42 MeV from the pair production of the gamma rays in the plastic scintillator. To achieve that, we applied an energy cut of $\pm 2\sigma$ around the annihilation peaks in the GAGG detectors. Figure 4 reveals the energy spectra of the GAGG detectors in triple timing coincidence with the plastic scintillator, showing the annihilation peaks in both detectors for all the runs combined.

During the initial test runs, we noticed a significant amount of rise in the bias current in the SiPM arrays coupled to our plastic scintillator, about 0.2 mA/day. SiPM damage by high neutron flux is well documented in the literature [6,7]. Hence, we were worried that our calibration source was damaging our equipment while possibly inducing dark current and noise [7]. Therefore, we placed 5 cm of borated polyethylene blocks between our detectors and the calibration source which ended up stopping the rapid rise of bias current in the SiPM.

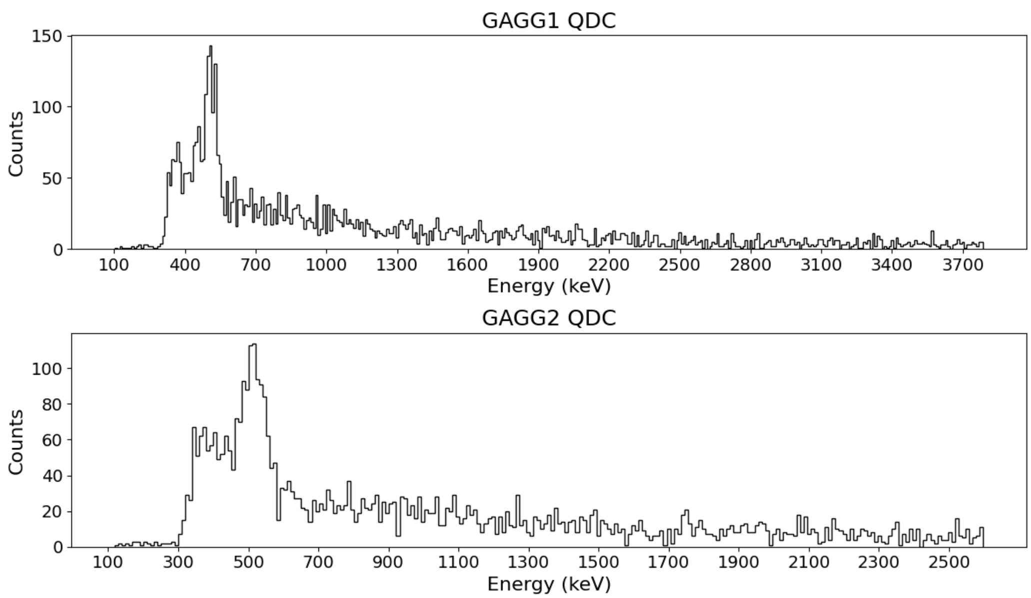

Fig. 4. The energy spectrum for both GAGG detectors after implementing the triple gamma-ray timing coincidence. The spectra clearly show the annihilation peaks around 511 keV.

4.2 Results

The isolated 3.42 MeV energy peak in the plastic detector is shown in Fig. 5. For these experiments, we note that we were restricted by statistics. Therefore, we had to count for several days. Here, we report our results for 88 hours of data in total.

Figure 5 also shows a Monte Carlo simulation for the 4.44 MeV gamma rays simulated on GEANT4. The simulation was convolved with a Gaussian function to take the detector resolution into account before being fitted to the experimental data. We notice a slight tail on the left-hand side of the energetic peak of the simulation due to bremsstrahlung escape from the electron-positron pairs created at the edge of the scintillator. However, the tail/peak ratio of the simulation is 0.13 which does not agree with the clearly bigger tail/peak ratio of the experimental data, as revealed in Fig. 5. Our GENAT4 simulation does not count non-uniform light collection and lower-energy neutrons entering the scintillator. Therefore, we associate the big tail on the left-hand side with neutron-induced events that mimic the annihilation radiation coincidence at 511 keV without generating the double-escape peak at 3.42 MeV.

Furthermore, we determined the energy resolution of the plastic detector at 3.42 MeV to be 11.5 ± 0.8% by fitting a Gaussian model to the double-escape peak.

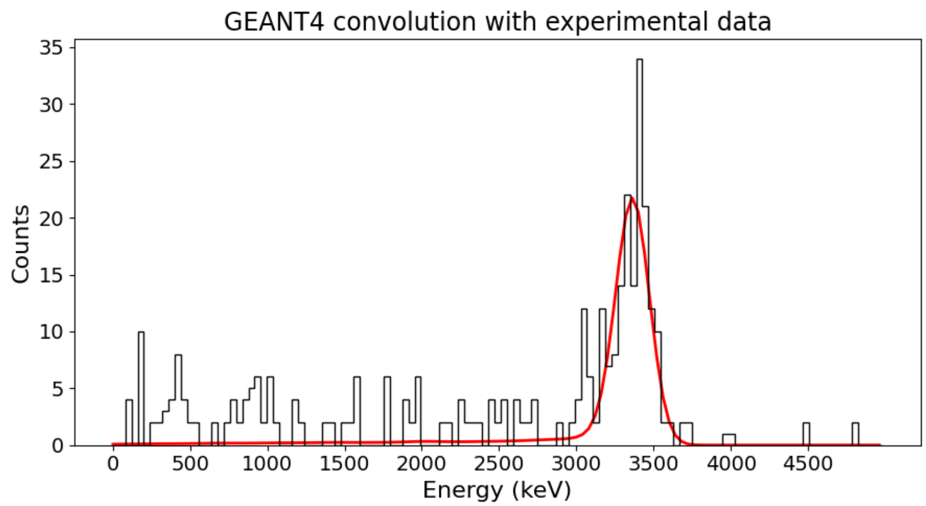

Fig. 5. The energy spectrum for the plastic detector shows the double escape peak at 3.42 MeV. The red solid line represents the GEANT4 simulation convolved with a Gaussian function.

5 45K Test Runs

We conducted two test experiments with the radioactive beam obtained from the proton beamline at TRIUMF and trapped a radioactive potassium isotope, 45K. Detected decay products were used to test the symmetry of the apparatus through coincident particle pairs for TRV. Due to higher statistics, we analyzed recoil ion coincidences with gamma rays detected by the GAGG detectors that are gamma-ray detectors.

The coincidence spectra were constructed by implementing recoil ion-gamma ray timing coincidences. We only looked at the coincidences around the main gamma-ray photopeak of 45K at 1706 keV to avoid information from the background in our spectra. Figure 6a shows the coincidence spectrum for our first run in August with 45K recoil time-of-flight (TOF) spectrum for the 45K decays to the 3/2 excited state for charge states +1 and +2 fitted to the experimental data. As seen in the figure, the recoil ion – gamma pair was not clean enough to test the apparatus symmetry for TRV. We report that the background dominates the coincidence spectrum even after the energy cuts around the main photopeak at 1706 keV.

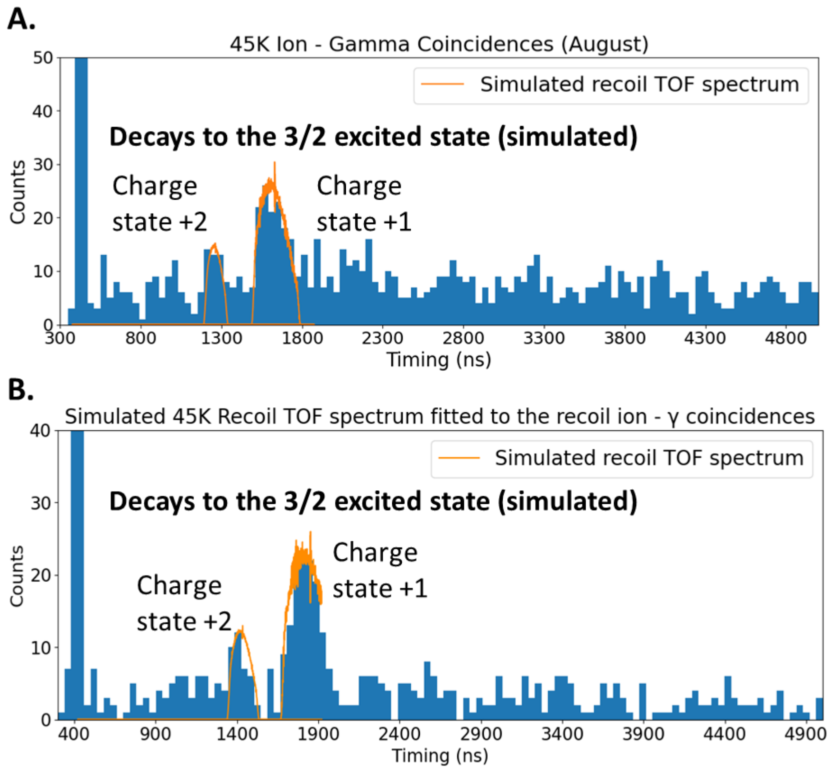

Fig. 6. 45K recoil ion – gamma ray coincidence spectrum for the **A.** August run and **B.** December run. The orange lines represent the TOF simulations for the decays of the recoil 45K to the 3/2 excited state for charge states +1 and +2.

On the contrary, Fig. 6b reveals the same spectrum collected during the December run with a better signal-to-noise ratio. We attribute this result to the improvements achieved in our experimental setup between the two runs, such as better atom trap light polarization and a much lower electron background from our microchannel plates.

6 Conclusion

We performed calibration and optimization studies for scintillation detectors to achieve high precision measurements required for TRV search in radiative beta decay in trapped atoms. We measured an energy resolution of 21.0 ± 0.7% at around 1 MeV for a plastic scintillator attached to a light guide which showed that the light guide significantly damages the energy resolution of the detector. We achieved an energy resolution as good as 9.3 ± 0.3% with the gain adjustments with a new housing design ensuring a light seal and tight contact between the SiPM array and the scintillator surface. We also measured an energy resolution as good as 10.1 ± 0.3% for our desired energy range of 0.5 – 5 MeV. Furthermore, a higher energy calibration method was introduced for plastic scintillation detectors using a neutron source, AmBe, and two inorganic GAGG detectors. Through triple gamma-ray timing coincidence and energy cuts around the annihilation radiation at 511 keV on the GAGG detectors, we were able to isolate the double-escape peak at 3.42 MeV on the plastic detector and measured an energy resolution of 11.5 ± 0.8%. Finally, we investigated our apparatus symmetry by analyzing the recoil ion coincidences with gamma rays during the radioactive test runs with trapped 45K atoms. We managed to improve the signal-to-noise ratio on the coincident particle pair spectrum in the second run through improvements in our atom trap. The particle coincidence results are significant for future TRV studies.

References

[1] Gardner, Susan, and Daheng He. "Radiative β decay for studies of CP violation." Physical Review D 87.11 (2013): 116012.

[2] https://trinat.triumf.ca/

[3] Janecek, M. “Reflectivity Spectra for Commonly Used Reflectors.” IEEE Transactions on Nuclear Science, vol. 59, no. 3, 2012, pp. 490–97, https://doi.org/10.1109/TNS.2012.2183385.

[4] Genat, Jean-Francois, et al. "Signal processing for picosecond resolution timing measurements." Nuclear Instruments and Methods in Physics Research Section A: Accelerators, Spectrometers, Detectors and Associated Equipment 607.2 (2009): 387-393.

[5] M.E. Rose: "Theory of Internal Conversion", in: Alpha-, Beta- and Gamma-Ray Spectroscopy, ed. by Kai Siegbahn, North-Holland Publishing, Amsterdam (1966), Vol. 2

[6] Ulyanov, Alexei, et al. "Radiation damage study of SensL J-series silicon photomultipliers using 101.4 MeV protons." Nuclear Instruments and Methods in Physics Research Section A: Accelerators, Spectrometers, Detectors and Associated Equipment 976 (2020): 164203.

[7] Musienko, Yu, et al. "Radiation damage in silicon photomultipliers exposed to neutron radiation." Journal of Instrumentation 12.07 (2017): C07030.